Available online at www.sciencedirect.com
SCIENCE DIRECT
Catalysis Today 102–103 (2005) 78–84
CATALYSIS TODAY
www.elsevier.com/locate/cattod

Hydrogen production by ethylene decomposition over Ni supported on novel carbon nanotubes and nanofibers

P.G. Savva [a], G.G. Olympiou [a], C.N. Costa [a], V.A. Ryzhkov [b], A.M. Efstathiou [a,*]

[a] *Chemistry Department, University of Cyprus, P.O. Box 20537, CY1678 Nicosia, Cyprus*
[b] *Rosseter Holdings Ltd., P.O. Box 57220, Limassol, Cyprus*

Available online 25 March 2005

Abstract

Ethylene decomposition over Ni supported on novel carbon nanotubes (CNT) and nanofibers under consecutive reaction/regeneration cycles to form CO-free hydrogen and carbon deposits have been investigated. The present work highlights the effects of support chemical composition, catalyst synthesis method and Ni metal loading on the catalytic activity and stability of nickel. A novel 0.5 wt.% Ni/CNT catalyst which presents the highest value of a constant hydrogen product yield (17.5 mol H_2/mol Ni), following consecutive reaction (complete deactivation) → regeneration (20% O_2/He, 400 °C) cycles, ever reported in the open literature has been developed. Transmission electron microscopy (TEM) and XRD studies revealed that the 0.5 wt.% Ni/CNT catalyst promotes the formation of two types of carbon nanofibers during ethylene decomposition at 400 °C, result that reduces significantly the rate of Ni encapsulation during reaction. The opposite is true in the case of 0.3 wt.% Ni/SiO_2 catalyst. In the case of Ni/CNT, there is a narrow range of Ni loading for which maximum H_2 product yield is obtained, while in the case of Ni/SiO_2, a monotonic increase in the H_2 product yield is obtained (Ni loading in the range 0.3–7.0 wt.%).

Keywords: Ni/CNF; Ni/SiO_2; C_2H_4 decomposition; Gasification of carbon nanofibers; Carbon nanotubes

1. Introduction

Hydrogen is expected to become an important energy carrier for sustainable energy consumption with a significantly reduced impact on the environment. Hydrogen fuel-cell is the most pronounced example. However, conventional processes of hydrogen production, such as steam reforming and partial oxidation of natural gas result in the simultaneous production of CO and CO_2, where the emissions of the latter have to be significantly reduced according to the recent Kyoto agreement [1]. Clean production of hydrogen is possible by water electrolysis using renewable energy sources (e.g., solar energy). However, this process is not competitive considering the current energy costs. Thus, alternative routes for the production of CO-free hydrogen become necessary for fuel-cell applications (e.g., PEM cells). Methane decomposition into hydrogen and carbon has taken most of the attention so far, and several attempts have been reported [2–7]. Economic analysis has shown that if the carbon produced can be recovered and utilized, this approach could be financially attractive [8].

Transition metals, such as Ni, Pd and Co, showed significant catalytic activity towards the direct decomposition of methane. However, the main problem of this catalytic process is the relatively rapid deactivation of the catalyst that is associated with carbon build-up. The latter causes reactor blocking and the need for catalyst regeneration. A suitable catalyst for the direct decomposition of hydrocarbons must present a highly sustainable activity and regeneration capability. One of the key important parameters to meet these requirements is the choice of a proper support chemical composition for the dispersion of transition and/or noble metal (e.g., Ni and Pd) [2,6] and the use of appropriate regeneration conditions (gas and temperature treatment) [5–7].

The present work concerns fundamental studies on the direct decomposition of ethylene over Ni supported on novel carbon nanotubes (CNT) recently patented [9]. Even though

* Corresponding author. Tel.: +357 2 2892776; fax: +357 2 2892801.
E-mail address: efstath@ucy.ac.cy (A.M. Efstathiou).

0920-5861/$ – see front matter © 2005 Elsevier B.V. All rights reserved.
doi:10.1016/j.cattod.2005.02.008

methane is the most abundant hydrocarbon (natural gas) and has the highest H/C ratio, other hydrocarbons that are produced by other fuel feedstocks (e.g., naphtha) could be considered. For example, ethane and ethylene whose growth production is expected to increase and their catalytic production technology is well established. It is reasonable to expect that the rate of H_2 production by the catalytic cracking of CH_4 and C_2H_4 and the ease of catalyst regeneration will be strongly determined by the C–H bond strength and the type of carbon formed for the two reactions.

The production of pure hydrogen by direct catalytic decomposition of ethylene over Ni supported on CNT is reported for the first time. This work provides important information concerning the effects of support chemical composition, catalyst synthesis method and Ni metal loading on catalyst activity (mols H_2/g Ni) and stability towards ethylene decomposition followed by catalyst regeneration for carbon removal.

2. Experimental

2.1. Catalyst preparation

The novel carbon nanotubes (coded as Ros1 and Ros5) used as supports of Ni metal were supplied by Rosseter Holdings Ltd. [9]. The Ros1 consists of 50–80% multi-walled nanotubes and 20–50% carbon polyhedral nanoparticles and disordered graphite, while the Ros5 mainly of disordered graphite. Both supports were calcined at 250 °C in air for 4 h before metal deposition was taken place. The SiO_2 support used was of standard grade (99.6% purity, Aldrich).

The supported metal catalysts (x wt.% Ni/support) were prepared by the incipient wetness impregnation method using $Ni(acac)_2{\cdot}4H_2O$ (99%, Aldrich) and $Ni(NO_3)_2{\cdot}6H_2O$ (Aldrich) salts as metal precursors and water as a solvent. After impregnation and drying (overnight at ~120 °C), the catalyst samples were calcined in air at 300 °C for 2 h and then reduced in pure H_2 at 300 °C for 2 h before any measurements were taken.

2.2. Catalyst characterization

2.2.1. Metal dispersion measurements

Metal dispersion of the catalysts was determined by H_2 chemisorption followed by temperature-programmed desorption (TPD) in He flow according to the following procedure. The catalyst was first oxidized in 20% O_2/He gas mixture at 300 °C for 2 h and then reduced in 20% H_2/He gas mixture at 300 °C for 2 h. Following this pretreatment, the catalyst was heated to 500 °C in He flow in order to desorb any H_2 that might spilt-over the support. The catalyst sample was then cooled in He flow to 150 °C. The feed was then switched to a 2% H_2/He gas mixture for 30 min. After this adsorption step, the catalyst was cooled in 2% H_2/He to room temperature and left for 15 min. The feed was then switched to He for 15 min and the temperature of the catalyst was increased to 600 °C to carry out a TPD experiment.

2.2.2. XRD analyses

The crystal structure of the fresh and used 0.5 wt.% Ni/Ros1 catalysts and the Ros1 (CNT) support were checked by XRD (SIEMENS Diffract 500 system, Cu Kα radiation (λ = 1.5418 Å)).

2.2.3. Transmission electron microscopy (TEM) measurements

TEM studies were performed over the 0.5 wt.% Ni/Ros1 and 0.3 wt.% Ni/Ros5 catalysts as prepared, after 14 and 3 h of continuous ethylene decomposition reaction (until complete deactivation), respectively, and after regeneration conditions were applied. Also, TEM micrographs were obtained on the 0.3 wt.% Ni/SiO_2 catalyst after 1 h of continuous ethylene decomposition reaction (until complete deactivation). The fresh catalysts were calcined in air at 400 °C for 2 h and then reduced in H_2 at 300 °C for 2 h before TEM measurements were performed. A 5-mg powder sample was dispersed in 1 ml of methanol and kept in an ultrasonic bath for 1 h. The sample was then deposited on a copper grid and dried at 25 °C. The instrument used was a JEOL 1010 electron microscope operated at an acceleration voltage of 80 kV.

2.3. Catalytic studies

The gas flow system used for conducting catalytic measurements at 1 atm total pressure consisted of a mass flow measuring and control system (MKS Instruments, Model 247C), mixing chambers, a quartz fixed-bed micro-reactor (2 ml nominal volume), and a GC/MS (Hewlett-Packard 5890, Series II Plus/Omnistar-Balzers) analysis system. The flow system, the micro-reactor and the analysis system used have been described in detail [10]. The feed stream consisting of 1.12% C_2H_4 in He was used in all catalytic experiments. The amount of supported-Ni catalyst sample used for catalytic experiments was 30 mg diluted in 120 mg of SiO_2 (150 mg of total bed mass) and the total flow rate was 50 N ml/min, resulting in a GHSV of about 200,000 h^{-1}. The regeneration of the used (completely deactivated) supported-Ni catalyst was carried out as follows. Initially, the deactivated catalyst sample was treated in a 20% O_2/He gas mixture at 400 °C and the CO (m/z = 28) and CO_2 (m/z = 44) signals were recorded continuously by on line mass spectrometer. Oxidation was considered complete if no further CO and CO_2 production was observed. The catalyst sample was then reduced by H_2 pulses at 400 °C, until no further consumption of hydrogen was noticed. A subsequent reaction/regeneration cycle was then initiated. The amount of hydrogen used in the pulsing mode was found to be about 0.18 mols H_2/g Ni in the case of

0.5 wt.% Ni/Ros1-a catalyst. This amount is about 1% of the hydrogen produced in every reaction cycle.

The hydrogen product yield (mols H_2/g Ni) was estimated by integrating the H_2 gas phase transient response at the exit of the microreactor continuously recorded with the mass spectrometer, and using the Ni loading of the catalyst prepared. The amount of carbon (g C/g Ni) was estimated by performing a carbon material balance based on the continuous recording of C_2H_4 signal with mass spectrometer and any CO_x or other hydrocarbons likely formed (use of MS/GC). It should be noted here that no such gaseous species were found. Therefore, the carbon analysis based solely on the ethylene signal was very accurate. Indeed, the carbon and hydrogen material balances closed within 3–7%, indicating that the carbon accumulated on the catalyst contained very little hydrogen, if any.

3. Results and discussion

3.1. Transient ethylene catalytic decomposition—effect of support

Fig. 1(a) presents the H_2 product concentration (mol%) obtained on 0.3 wt.% Ni supported on Ros1, Ros5 and SiO_2 solids after reaction with a 1.12 mol% C_2H_4/He gas mixture at 400 °C as a function of time on stream. It should be noted that no other gaseous products besides H_2 were observed in the present experiments. The catalysts with the (-n) suffix (e.g., Ni/Ros1-n) were prepared using the Ni nitrate precursor, while that with the (-a) suffix was prepared using the Ni acetate precursor. As shown in Fig. 1(a), the Ni/Ros1-n presents the highest initial catalytic activity among the other catalysts investigated. In addition, the same catalyst exhibits twice the lifetime and a much larger H_2 product yield (4.1 mols H_2/g_{Ni}) than the Ni/SiO_2-n and Ni/Ros5-n catalysts (1.7 and 1.0 mols H_2/g_{Ni}, respectively). On the other hand, the Ni/Ros1-a appears to have a significant sustainable catalytic activity (about 14 h of continuous reaction, 12.9 mols H_2/g_{Ni} until complete deactivation) as opposed to the Ni/Ros1-n catalyst.

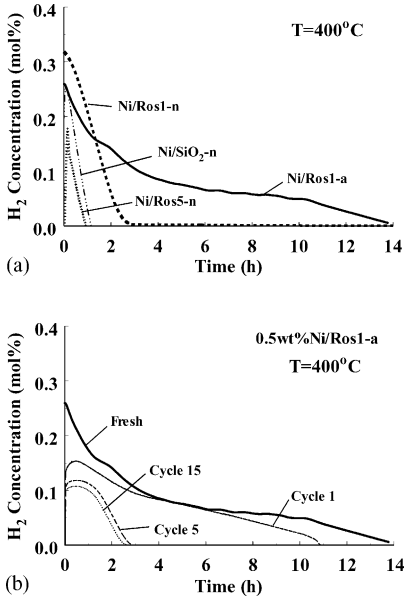

Fig. 1. H_2 product concentration as a function of time on stream following reaction of 1.12 mol% C_2H_4/He at 400 °C (GHSV = 40,000 h^{-1}) over 0.3 wt.% Ni/Ros1-a, 0.3 wt.% Ni/Ros1-n, 0.3 wt.% Ni/SiO_2 and 0.3 wt.% Ni/Ros5-n catalysts.

According to previous works [2,6,11–14], on CH_4 decomposition reaction, the results presented in Fig. 1(a) could be attributed to the different kinds of carbon formed by the ethylene decomposition, the latter influenced by the Ni particle size and morphology (e.g., exposed crystallographic planes and surface electronic structure). In turn, the latter parameters are influenced by the chemical composition of the support and the nature of metal precursor used. According to TEM and XRD studies to be presented later on, different types of carbon were formed by the Ni/Ros1-a, Ni/Ros5-n and Ni/SiO_2 catalysts. While in the case of the former catalyst carbon nanofibers (CNFs) were formed, in the case of Ni/SiO_2 and Ni/Ros5-n no filamentous carbon was formed but rather graphitic carbon. In the case of methane decomposition over supported Ni particles, it is now well established that a Ni particle produces a carbon nanofiber of the same size as itself by adsorption of the methane molecule followed by its decomposition into hydrogen and carbon atoms on the Ni surface, diffusion of the carbon atoms on the Ni surface and in the bulk of Ni particle to the precipitation sites (the metal–support interface), where they are crystallized to form a graphitic layer, the latter being the starting growth of a carbon nanofiber, with the exposed Ni particle as its tip [6,15].

Therefore, the promotion of CNFs formation during ethylene decomposition results in the prolong extent of catalytic activity towards H_2 formation. It is mentioned here that the Ros1 support contains about 0.05–0.1 wt.% Fe in the form of nanoparticles (average $d \sim 1.5$ nm) [9]. It is speculated whether these Fe clusters are also responsible for the prolonged catalytic activity of Ni/Ros1-a catalyst. Further work is in progress to address this important issue.

The present catalysts reported in Fig. 1(a) have similar Ni dispersions (∼60%). This could imply that the Ni particle size is not connected to the transient catalytic activity reported in Fig. 1(a). However, as will be shown in the following Section 3.2, the Ni particle size in a narrow range strongly affects the catalytic activity of ethylene decomposition. Similar dispersions do not necessarily imply the same Ni particle size distribution. It is therefore suggested that differences in Ni particle size distribution among all four supported-Ni catalysts presented in Fig. 1(a) could be another important factor for determining their transient catalytic activity. The large differences in the transient catalytic activity behaviour exhibited by Ni/Ros1-a and Ni/Ros1-n is most likely due to the different Ni particle size distribution established by the Ni metal precursor used in the

wetness impregnation method. It is expected that the hydration and coordination sphere of Ni^{2+} in aqueous solution with the presence of nitrates or acetate ions will be different. The latter will affect the adsorption mode of nickel ions on the Ros1 surface and the final size distribution of Ni clusters formed.

Fig. 1(b) illustrates the effect of regeneration of the catalyst on the transient kinetics of hydrogen production as a function of the number of regeneration cycles performed over the 0.5 wt.% Ni/Ros-1a catalyst, the best developed in the present work. It is clearly observed that there is a progressive change in the transient kinetics of hydrogen production, until the fifth reaction/regeneration cycle. Further results on this subject will be presented and discussed in the following Section 3.3.

3.2. Effect of Ni loading

Fig. 2 presents the effect of Ni loading in the 0.15–10 wt.% range for nickel supported on Ros1-a (Fig. 2(a)) and SiO_2 (Fig. 2(b)), respectively, on the total H_2 production per gram of Ni (until complete catalyst deactivation) for the reaction at hand. As shown in Fig. 2(a), the H_2 production goes through a maximum at a Ni loading of 0.5 wt.%. On the contrary, the increase of Ni loading in the case of SiO_2-supported Ni catalyst results in an increase of the amount of H_2 produced per gram of Ni. This behaviour is suggested to be largely due to the effect of Ni particle size. It is noted that a Ni dispersion of about 10% was measured in the case of 10 wt.% Ni compared to 60% in the case of 0.3 wt.% Ni for the Ni/Ros1-a catalytic system.

Takenaka et al. [2,11] have recently reported results concerning the methane decomposition reaction over Ni/SiO_2 and Pd-Ni/CF (carbon fiber) catalysts. The authors

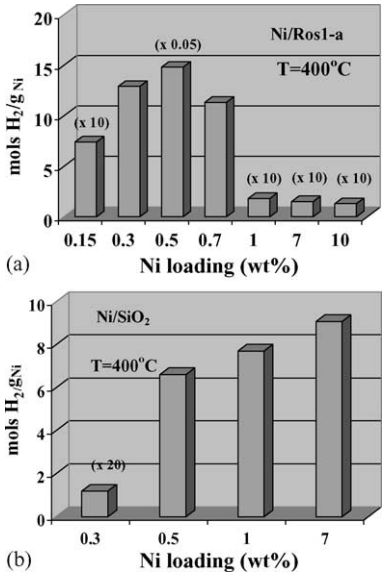

Fig. 2. Effect of Ni loading on the production of H_2 following reaction of 1.12 mol% C_2H_4/He at 400 °C (GHSV = 200,000 h^{-1}) over (a) *x* wt.% Ni/Ros1-a and (b) *x* wt.% Ni/SiO_2-n catalysts.

have reported that the amount of carbon formed by the reaction was significantly dependent on the nickel metal loading. In particular, it was shown that the methane decomposition reaction over Pd-Ni/CF is favoured at low metal loadings and that the H_2 yield (per gram of Ni) over Ni/SiO_2 also increased with increasing Ni loading in the 1–40 wt.% range. The same authors have proposed that Ni metal particles with diameter in the 60–100 nm range are the most effective ones for methane decomposition into H_2.

It is important to note at this point that the hydrogen yield value of 296 mols H_2/g_{Ni} obtained over the 0.5 wt.% Ni/Ros1-a catalyst (Fig. 2(b)) is the highest one ever reported in the open literature for both the CH_4 and C_2H_4 decomposition reactions. This remarkable catalytic behaviour of Ni/Ros1-a catalyst is illustrated in Table 1 in terms of total carbon capacity (g_C/g_{Ni}) and H_2 production (mol H_2/mol Ni) for the most active catalysts reported in the literature for methane decomposition. According to the results of Table 1, the Ni/Ros1-a catalyst appears to be superior in all respects of its performance to all other Ni- and Pd-Ni-based catalysts. In particular, the 0.5 wt.% Ni/Ros1-a presents about 2.5 times higher H_2 production and carbon capacity values (per mol of metal) compared to the Pd-Ni/CF catalyst. According to the literature, the latter catalyst is considered to be the most active one reported so far for the methane decomposition reaction [2].

As mentioned above, the results presented in Fig. 2 are likely to be due to the influence of chemical composition of support on the nickel particle size and morphology, parameters that would determine the surface nickel electronic structure, and therefore its chemisorptive and catalytic properties [11–13]. The remarkable catalytic results obtained over the Ni/Ros1-a catalyst are mainly due to the influence of the chemical composition of support on the catalytic properties of Ni metal that promote the catalytic steps of ethylene decomposition and of the carbon or carbonaceous species (e.g., C_xH_y) formation mechanism and structure on the catalyst surface. The alteration of the catalytic properties of supported-Ni catalysts could be explained in terms of the ensemble (geometric) and electronic factor [16]. The geometric factor implies formation of nickel clusters of a certain size on the surface of support, while the electronic factor concerns the modification of electronic properties of Ni due to electronic interactions with the support. According to Alstrup and Tavares [17], methane decomposition and carbon growth over nickel catalysts includes the steps of activation and decomposition of methane on (1 0 0) and (1 1 0) Ni surface planes. The latter suggests that the initial activity of supported-Ni catalysts towards methane and possibly ethylene decomposition reactions strongly depends on the surface crystallographic structure of the Ni particles, which in turn is significantly affected by the chemical composition of support [17]. In addition, Park and Keane [12] have reported that the structure of the carbon species deposited on supported-Ni catalysts during ethylene decomposition is

Table 1
Catalytic activity of various supported-Ni and Pd-Ni catalysts for the methane decomposition reaction in the 400–625 °C range

Catalyst	Feed conditions			Carbon capacity g_C/g_{Ni}	H_2 production, H_2/Ni (mol/mol) $\times 10^{-3}$	References
	y_{CH_4}	T (°C)	GHSV (h^{-1})			
90% Ni/SiO_2	1	550	1200	384	1.88	[13]
75% Ni-15% Cu/Al_2O_3	1	625	300	700	3.44	[16]
10% Ni/ZSM-5	0.2	450	15,000	280	1.37	[18]
40% Ni/SiO_2	1	500	180,000	491	2.40	[11]
23% Pd-23%Ni/CF	1	600	300,000	1424[a]	7.00[b]	[2]
0.5% Ni/Ros1-a	0.0112[c]	400	200,000	3552	16.57	This work

[a] Per gram of total metal (Ni + Pd).
[b] Per mol of total metal (Ni + Pd).
[c] Results concern the ethylene decomposition reaction (1.12 mol% C_2H_4/He).

strongly influenced by the nature of support. In particular, the authors reported that Ni metal fragments are formed during ethylene decomposition reaction which promotes a secondary (narrower) fiber growth compared to the initial one. It is reported that the diameter of these produced carbon fibers strongly depends on the size of the supported Ni particles. In the case of the catalysts with low metal loadings (smaller Ni particles), these branched carbon ribbons appear like amorphous in low-resolution TEM images and XRD patterns. The latter effect that particularly prevails in the case of Ni supported on activated carbon (AC) results in the prolonged stability of Ni/AC compared to the rest of the catalysts examined [12].

Fig. 3(a) and (b) show TEM micrographs of the 0.5 wt.% Ni/Ros1-a catalyst as fresh and after 14 h of continuous ethylene decomposition, respectively. It appears that the used catalyst presents much more branched carbon nanofibers compared to the fresh one. Based on XRD measurements and analyses, two kinds of carbon fibers were formed. The thinner ones resemble the herringbone carbon nanofiber structure with $d_{0\,0\,2} = 0.345$–0.35 nm, while the thicker ones which were the most abundant resemble the structure of well-graphitized platelet carbon nanofibers ($d_{0\,0\,2} = 0.335$ nm). Also, based on similar TEM measurements performed on Ni/Ros-5 and Ni/SiO_2 catalysts as fresh and after ethylene decomposition reaction, these catalyst compositions do not favour the formation of carbon nanofibers. It is therefore concluded that formation of carbon nanofiber structures reduces the rate of Ni encapsulation as ethylene decomposition reaction proceeds, while the opposite is true in the case of graphitic carbon.

3.3. Effects of regeneration cycles on catalytic activity

One of the most crucial parameters that have to be taken into account for the critical evaluation of a catalyst's performance in the case of hydrocarbon decomposition reactions is the catalyst ability to regain all or a significant part of its initial activity after proper regeneration procedures (sustainable catalytic activity). Fig. 4 compares the catalytic activity in terms of total H_2 production (mols H_2/g_{Ni}) of the fresh and regenerated 0.5 wt.% Ni/Ros1-a catalyst after ethylene decomposition at 400 °C. A significant gain (>70%) in H_2 product yield can be achieved during the first regeneration cycle. However, the gain in the

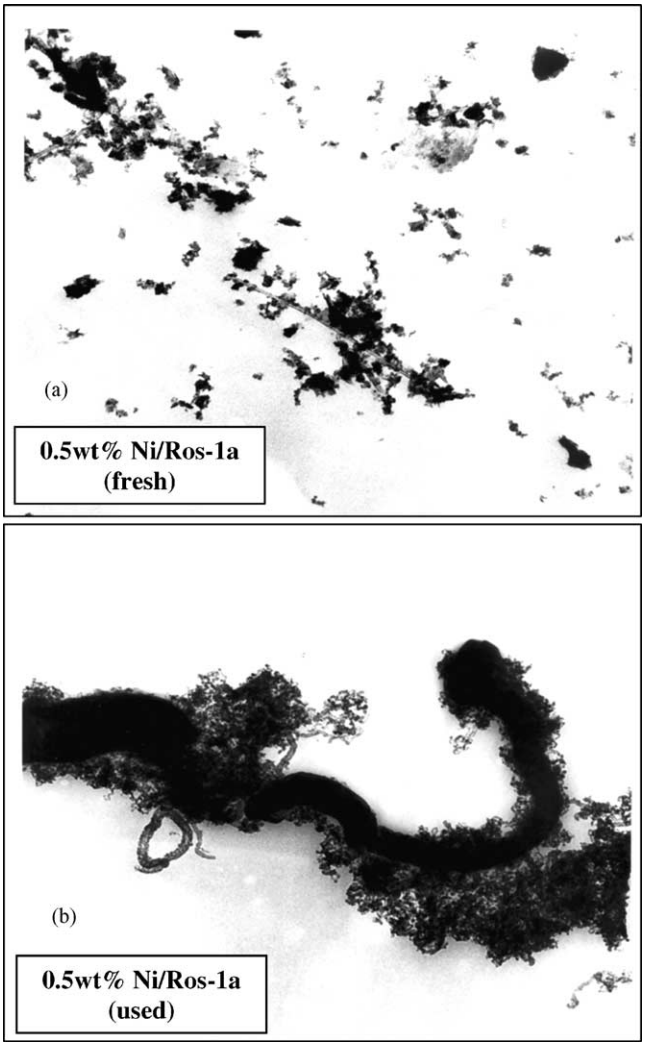

Fig. 3. Transmission electron microscopy (TEM) photographs obtained on (a) the fresh 0.5 wt.% Ni/Ros1-a catalyst and (b) the 0.5 wt.% Ni/Ros1-a used for 14 h of continuous ethylene decomposition reaction at 400 °C. Reaction conditions: feed gas composition of 1.12 mol% C_2H_4/He; GHSV = 200,000 h^{-1}.

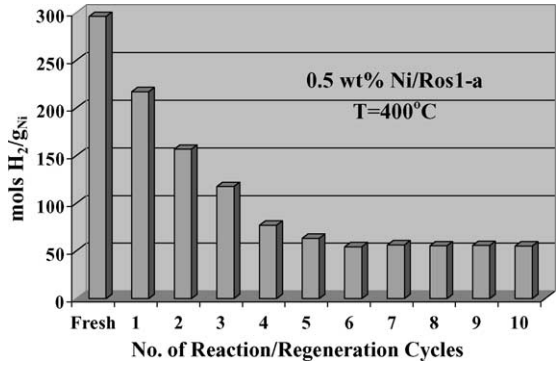

Fig. 4. H_2 product yield (mols H_2/g_{Ni}) obtained after performing consecutive reaction/regeneration cycles over the 0.5 wt.% Ni/Ros1-a catalyst at 400 °C. Reaction conditions: feed gas composition of 1.12 mol% C_2H_4/He; GHSV = 200,000 h^{-1}.

catalyst initial activity decreases during the first five reaction/regeneration cycles. On the other hand, the catalyst appears to be remarkably stable after the fifth reaction/regeneration cycle. After the 10th consecutive reaction/regeneration cycle, the Ni/Ros1-a catalyst presents a total H_2 production value of 56 mols H_2/g_{Ni}, which is the highest value ever reported in the literature for both methane and ethylene decomposition reactions over supported-Ni catalysts. It is noted that without performing the H_2 reduction step after regeneration with 20% O_2/He gas mixture of the fully deactivated catalyst, the H_2 product yield was found to be about half of that obtained with the H_2 reduction step between successive reaction/regeneration cycles. This is a very important result from a practical point of view, since no H_2 consumption is required for the H_2 reduction step of the oxidized Ni catalyst between regeneration and subsequent reaction step. Takenaka et al. [6] have studied the regeneration of supported-Ni catalysts after CH_4 decomposition at 550 °C by using CO_2 instead of oxygen at 650 °C without any intermediate reduction step of the catalyst. Their results have indicated that gasification of the deposited carbon with CO_2 resulted in the selective formation of CO as well as the regeneration of the deactivated catalyst. Studies addressing CO_2 and H_2O regeneration of the present Ni/Ros1-a catalyst after C_2H_4 decomposition reaction are currently under way.

TEM and XRD measurements performed on the regenerated 0.5 wt.% Ni/Ros1-a catalyst after the first reaction/regeneration cycle have shown that much shorter branches of produced carbon nanofibers compared to the used catalyst were present. Also, only the thinner carbon nanofibers remained on the catalyst surface. These results could explain very well the results of Fig. 4. The initial activity loss is due to the fact that some Ni active sites are encapsulated by the carbon formed on the catalyst, where not all of it is gasified by the applied O_2/He regeneration conditions. It is speculative whether the consecutive reaction/regeneration cycles have also altered the morphology of the Ni particles. Based on H_2 chemisorption measurements, the Ni dispersion of the fresh catalyst (∼60%) was reduced to 47% after the fifth reaction/regeneration cycle. These results at least show that there should not be a significant effect of Ni particle size on the activity results described in Fig. 4.

4. Conclusions

The present work reports on the development of a novel Ni catalyst supported on CNT (0.5 wt.% Ni/Ros1-a) for the direct decomposition of ethylene at 400 °C to produce CO-free hydrogen. This catalytic system presented the highest hydrogen yield (mols H_2/g_{Ni}) and carbon capacity (g_C/g_{Ni}) ever reported in the literature for both the ethylene and methane decomposition reactions. In particular, the 0.5 wt.% Ni/Ros1-a catalyst exhibited 50 times higher hydrogen yield compared to a 0.3 wt.% Ni/SiO_2 catalyst which has been examined under the same experimental conditions.

The catalytic performance of the Ni/Ros1-a catalyst was found to strongly depend on the Ni metal loading. A 0.5 wt.% Ni is approximately an optimum metal loading in the 0.15–10 wt.% range investigated. The 0.5 wt.% Ni/Ros1-a catalyst prepared from a nickel acetate precursor showed significantly better catalytic activity than the one prepared using nickel nitrate as a metal precursor.

It was found that a significant (>70%) gain in the H_2 product yield can be achieved by the use of 20% O_2/He at 400 °C regeneration conditions over the 0.5 wt.% Ni/Ros1-a catalyst. The presently developed Ni/Ros1-a catalyst showed remarkable activity, the highest ever reported, after 10 consecutive reaction/regeneration cycles performed with 14-h reaction duration for each regeneration cycle.

Acknowledgements

Financial support by the Research Committee of the University of Cyprus is gratefully acknowledged. The research group of Dr. K. Kyriakou at the Cyprus Institute of Neurology is also acknowledged for performing the TEM measurements.

References

[1] The Kyoto Protocol 2002, United Nations Conference on Greenhouse Emissions, Kyoto, Japan (1997).
[2] S. Takenaka, Y. Shigeta, E. Tanabe, K. Otsuka, J. Catal. 220 (2003) 468.
[3] K. Otsuka, H. Ogihara, S. Takenaka, Carbon 41 (2003) 223.
[4] J.I. Villacampa, C. Royo, E. Romeo, J.A. Montoya, P. Del Angel, A. Monzón, Appl. Catal. A: Gen. 252 (2003) 363.
[5] S. Takenaka, Y. Tomikubo, E. Kato, K. Otsuka, Fuel 83 (2004) 47.
[6] S. Takenaka, E. Kato, Y. Tomikubo, K. Otsuka, J. Catal. 219 (2003) 176.
[7] R. Aiello, J.E. Fiscus, H.-C. zur Loye, M.D. Amiridis, Appl. Catal. A: Gen. 192 (2000) 227.
[8] M. Steinberg, H.C. Cheng, Int. J. Hydrogen Energy 14 (1989) 797.
[9] V.A. Ryzhkov, The method and device for producing higher fullerenes and nanotubes, PCT/IB00/00406, 2000.

[10] C.N. Costa, T. Anastasiadou, A.M. Efstathiou, J. Catal. 194 (2000) 250.
[11] S. Takenaka, S. Kobayashi, H. Ogihara, K. Otsuka, J. Catal. 217 (2003) 79.
[12] C. Park, M.A. Keane, J. Catal. 221 (2004) 386.
[13] M.A. Ermakova, D.Y. Ermakov, G.G. Kuvshinov, L.M. Plyasova, J. Catal. 187 (1999) 77.
[14] N. Muradov, Catal. Commun. 2 (2001) 89.
[15] R.T.K. Baker, Carbon 27 (1989) 315.
[16] T.V. Reshetenko, L.B. Avdeeva, Z.R. Ismagilov, A.L. Chuvilin, A. Ushakov, Appl. Catal. A: Gen. 247 (2003) 51.
[17] I. Alstrup, M.T. Tavares, J. Catal. 139 (1993) 513.
[18] T.V. Choudhary, C. Sivadinarayana, C.C. Chusuei, A. Klinghoffer, D.W. Goodman, J. Catal. 199 (2001) 9.